Electrically tunable two-dimensional holographic photonic crystal fabricated by a single diffractive element

Y. J. Liu and X. W. Sun[a)]
School of Electrical and Electronic Engineering, Nanyang Technological University, Nanyang Avenue, Singapore 639798, Singapore

(Received 15 July 2006; accepted 6 September 2006; published online 23 October 2006)

An electrically tunable two-dimensional holographic photonic crystal was fabricated in polymer-dispersed liquid crystal using a single diffraction element, which was a specially designed photomask consisting of three diffraction gratings, which had a period of 4 μm, oriented 120° relative to one another. With the photomask subjected to a collimated Ar^+ laser beam operating at 514.5 nm, a two-dimensional spatial light intensity pattern was created by interference of the three first order diffracted beams produced by the mask. The spatial light intensity pattern was then recorded inside a cell filled with the liquid crystal/prepolymer mixture to create a photonic crystal. The photonic crystal structures were observed under an optical microscope. It showed triangular structures with a lattice constant of about 2.50 μm. The diffraction properties and electro-optic tunability were also presented. © *2006 American Institute of Physics*. [DOI: 10.1063/1.2364471]

Photonic crystals (PhCs) or photonic bandgap (PBG) materials, which enable the localization of light,[1,2] hold promise for an emerging generation of nano- and mesoscale optoelectronic components. Different approaches have been used to fabricate PhCs, such as electron-beam lithography,[3] self-organization of colloids,[4] layer-by-layer micromachining,[5] and holographic lithography.[6–10] Generally, a high refractive index contrast is required for a full PBG. However, materials with relatively low index contrasts, especially for organic materials, can also find applications that make use of their refraction properties, e.g., superprism effect.[11] Combining numerous desirable characteristics including one step, fast, large area fabrication, lattice tailor ability, and easy defect control, holographic photopolymerization offers a highly versatile approach to create organic PBGs.

Holographic polymer-dispersed liquid crystal (H-PDLC) material can be photopolymerized by UV or visible lasers.[12] It has attracted great attention not only for its physical properties but also for a wide range of potential applications, such as reflective flat-panel displays,[13–15] switchable lenses,[16] optical switches,[17,18] organic lasers,[19–21] etc. Recently, much interest is focused on fabricating PhCs based on H-PDLC. Many two- and three-dimensional (2D and 3D) PhCs have been demonstrated using H-PDLC materials, including transverse square,[22] orthorhombic,[23,24] and diamondlike lattices.[25] However, to achieve these structures, a relatively complicated optical setup is generally used to create multibeam interference pattern in all these fabrications.

In this letter, we will report an easy method to fabricate 2D H-PDLC PhCs only using a single diffraction element, a photomask, which creates a three-beam interference pattern. The mask is comprised of three diffraction gratings at 120° relative to one another. In our experiment, each grating on the mask has an area of 8×8 mm^2 and the grating period is 4 μm. Figures 1(a) and 1(b) show the schematic of the mask and three diffracted beams. This single mask implementation improves the alignment and stability of the optical setup, making it more robust than the multiple beam setups reported previously.

The starting LC/prepolymer mixture syrup used was consisted of 48 wt % monomer, trimethylolpropane triacrylate, 8 wt % cross-linking monomer, *N*-vinylpyrrollidone, 0.8 wt % photoinitiator, rose bengal, 1.2 wt % coinitiator, *N*-phenylglycine, 8 wt % surfactant, octanoic acid, all from Sigma-Aldrich, and 34 wt % liquid crystal E7 from Merck. The E7 liquid crystal used has an ordinary refractive index of $n_o=1.521$ and a birefringence of $\Delta n=0.225$. The detailed material processing for fabrication and morphology observation was reported previously.[18] An Ar^+ laser operating at 514.5 nm was used to produce the diffraction pattern. When a cell filled with the LC/prepolymer mixture is exposed to the diffraction pattern, the LC and polymer will redistribute due to the polymerization of the prepolymer induced by the light intensity, thus forming a 2D structure inside the cell.

The electrical field distribution of a multibeam interference can be generally described by

$$I(\boldsymbol{r}) = \left[\sum_{j=1}^{n} \boldsymbol{E}_j(\boldsymbol{r})\exp(i\boldsymbol{k}\cdot\boldsymbol{r}+i\phi_j)\right] \times \left[\sum_{j=1}^{n} \boldsymbol{E}_j^*(\boldsymbol{r})\exp(-i\boldsymbol{k}\cdot\boldsymbol{r}-i\phi_j)\right] = \sum_{j=1}^{n}|\boldsymbol{E}_j|^2 + \sum_{i\neq j}^{n}\boldsymbol{E}_i\cdot\boldsymbol{E}_j^*\exp[i(\boldsymbol{k}_i-\boldsymbol{k}_j)\cdot\boldsymbol{r}+i\phi_{ij}], \quad (1)$$

where $\boldsymbol{E}$ is the amplitude, $\boldsymbol{k}$ is the wave vector, i and j are positive integers, ϕ_{ij} is the initial phase difference between two incident waves, and $\boldsymbol{r}$ is the position vector. As reported before, all 14 Bravais lattices can be fabricated by recording four plane wave interference fringes.[9]

In our experiment, the beam vectors of the three diffracted first-order beams can be written as

$$\hat{\boldsymbol{k}}_1 = \sin\theta\cos\varphi_1\hat{\boldsymbol{e}}_x + \sin\theta\sin\varphi_1\hat{\boldsymbol{e}}_y + \cos\theta\hat{\boldsymbol{e}}_z, \quad (2)$$

a)Author to whom correspondence should be addressed; electronic mail: exwsun@ntu.edu.sg

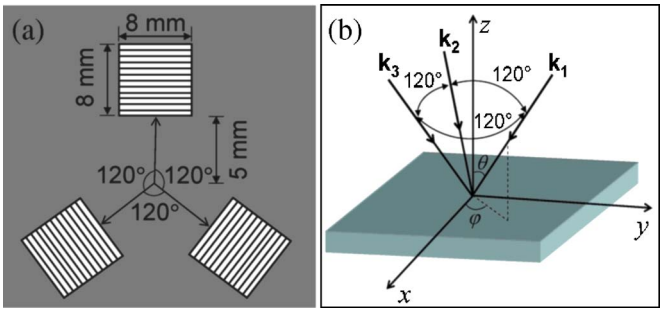

FIG. 1. (Color online) Schematics of the mask (a) and three first order diffracted beams (b).

$$\hat{\boldsymbol{k}}_2 = \sin\theta\cos\varphi_2\hat{\boldsymbol{e}}_x + \sin\theta\sin\varphi_2\hat{\boldsymbol{e}}_y + \cos\theta\hat{\boldsymbol{e}}_z, \tag{3}$$

$$\hat{\boldsymbol{k}}_3 = \sin\theta\cos\varphi_3\hat{\boldsymbol{e}}_x + \sin\theta\sin\varphi_3\hat{\boldsymbol{e}}_y + \cos\theta\hat{\boldsymbol{e}}_z, \tag{4}$$

where $\hat{\boldsymbol{k}}$ is a unit wave vector, $\hat{\boldsymbol{e}}$ is a unit coordinate vector, θ is the angle between the diffracted laser beam and z axis (the first order diffraction angle), and φ is the angle between the projection of laser beam on x-y plane and x axis [Fig. 1(b)]. Substituting Eqs. (2)–(4) into Eq. (1) with $\theta=7.4°$, $\varphi_1=180°$, $\varphi_2=-60°$, and $\varphi_3=60°$, we have

$$\begin{aligned} I &= (\boldsymbol{E}_1+\boldsymbol{E}_2+\boldsymbol{E}_3)\cdot(\boldsymbol{E}_1+\boldsymbol{E}_2+\boldsymbol{E}_3)^* \\ &= |\boldsymbol{E}_1|^2+|\boldsymbol{E}_2|^2+|\boldsymbol{E}_3|^2+2\boldsymbol{E}_1\cdot\boldsymbol{E}_2\cos\left(-\frac{3}{2}kx\sin\theta\right. \\ &\quad \left.+\frac{\sqrt{3}}{2}ky\sin\theta\right)+2\boldsymbol{E}_1\cdot\boldsymbol{E}_3\cos\left(-\frac{3}{2}kx\sin\theta\right. \\ &\quad \left.-\frac{\sqrt{3}}{2}ky\sin\theta\right)+2\boldsymbol{E}_2\cdot\boldsymbol{E}_3\cos(\sqrt{3}ky\sin\theta). \end{aligned} \tag{5}$$

With a three-beam intensity ratio of 1:1:1, the simulated 3D interference pattern is shown in Fig. 2. It is worth mentioning that the period of this triangular lattice equals to two-thirds of the diffraction grating period, i.e., 2.67 μm, which does not depend on the beam wavelength.[26] Therefore, the PBGs can be easily engineered by changing the grating period. Figure 3(a) shows an atomic force microscopy (AFM) image of the surface, which was obtained after LC was removed in ethanol. It reveals a clear hexagonal morphology with a lattice constant of about 2.5 μm, which is in good agreement with the simulation pattern (Fig. 2), considering

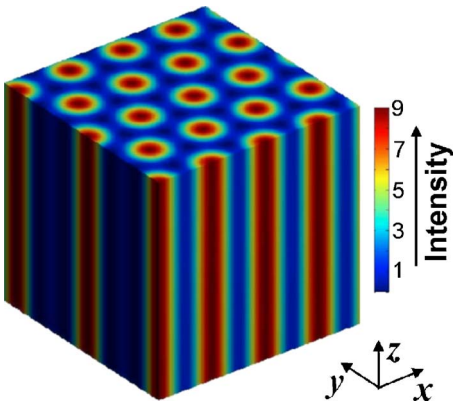

FIG. 2. (Color online) Simulated 3D interference pattern. The color bar shows the intensity distribution.

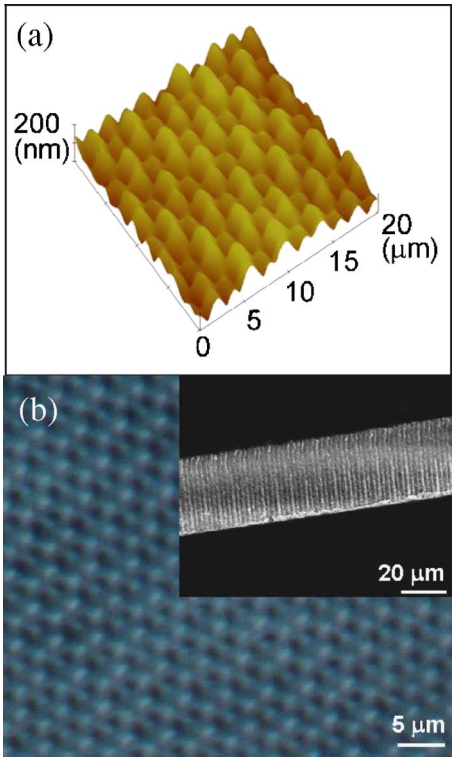

FIG. 3. (Color online) AFM (a) and optical microscopy (b) images showing the surface morphology of the 2D H-PDLC PhC and SEM image [the inset in (b)] showing the cross section morphology.

the general 5%–10% volume shrinkage for the acrylate monomer during the photoinduced polymerization.[11,19] It is interesting to note in Fig. 3(a), in a hexagonal cell, that the height of the central point is slightly different from its surrounding six points, which are almost the same in height. Figure 3(b) shows the surface morphologies of the 2D H-PDLC PhCs observed under a high resolution optical microscope. The inset scanning electron microscopy (SEM) image in Fig. 3(b) shows the cross section morphology of the sample, where columnar structure is clearly seen, which matches the simulation result in Fig. 2.

The diffraction patterns of the H-PDLC PhC were checked to confirm the quasicrystal structure. Figures 4(a) and 4(b) show the visible diffraction pattern produced by a normally incident He–Ne laser beam operating at 543 nm and a collimated broadband white beam for our H-PDLC PhC sample. From Fig. 4(a), we can see clear hexagonal diffraction spots which match well with our AFM, optical, and SEM images of a 2D hexagonal lattice (Fig. 3). The

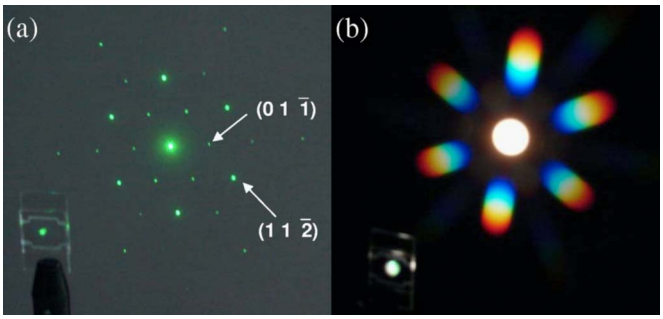

FIG. 4. (Color online) Visible diffraction patterns of the H-PDLC PhCs produced by a normally incident He–Ne laser beam (a) and a collimated broadband white beam (b).

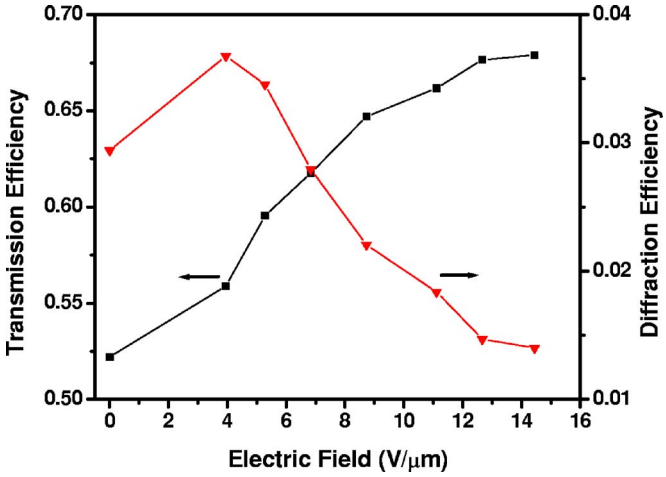

FIG. 5. (Color online) $(11\bar{2})$ diffraction efficiency and nondiffracted center beam transmission efficiency as functions of applied voltage.

diffracted spots originating from $(01\bar{1})$ and $(11\bar{2})$ surfaces are labeled in Fig. 4(a).[27] The images clearly reveal the presence of quasiperiodicity within the sample. The observed points are sharp and symmetrically distributed. As reported by Gorkhali *et al.*,[28] all diffraction points in the first and higher orders should show a N-fold symmetry and have $2N$ diffracted points, where N is the number of interference beams used to produce the PhC. For our case, $N=3$, in good agreement with the prediction, we can clearly see a threefold symmetry and six diffracted points for the same order of diffracted beams.

For the H-PDLC PhCs, a distinct advantage is that they can be tuned by applying a voltage, i.e., the PBGs of H-PDLC PhCs can be changed dynamically. Figure 5 shows the changes of the $(11\bar{2})$ diffraction efficiency and transmission efficiency (center beam without diffraction) as functions of applied voltage. The definitions of diffraction and transmission efficiencies can be found in Ref. 18. From Fig. 5, we can see that, with the increase of applied voltage, the $(11\bar{2})$ diffraction efficiency firstly increases and then decreases, while the transmission efficiency increases due to the refractive indices matching between the liquid crystal and polymer matrix. Optical clearing, originating from droplet size distribution, may be the possible reason for the initial increase in diffraction efficiency. In H-PDLC PhCs, large liquid crystal droplets tend to scatter more light, producing a haze effect. When an electric field is applied on the sample, these large droplets will align firstly due to the larger volume to surface area ratio, and the haze will disappear, thus, resulting in the diffraction efficiency increase initially. When the electric field continues to increase, the smaller droplets start to align, and the index modulation decreases. As a result, the diffraction efficiency will decrease. The $(11\bar{2})$ diffraction efficiency reduces by two times with an applied field of 14.5 V/μm (Fig. 5). Obviously, energy transfers from the higher order diffraction to the lower order diffraction happened because the higher order diffraction spots gradually disappeared with the increase of applied voltage.

In conclusion, electrically tunable 2D H-PDLC PhCs were fabricated using a single diffraction element. Such method offers single step, easy fabrication, and low cost compared with conventional lithography. The PhC structures can be easily engineered by designing different diffractive optical elements. Although due to the low refractive index contrast between the polymer and liquid crystal, such kind of H-PDLC PhCs cannot show complete PBGs, they can still find applications making use of their refraction properties.

[1] E. Yablonovitch, Phys. Rev. Lett. **58**, 2059 (1987).
[2] S. John, Phys. Rev. Lett. **58**, 2486 (1987).
[3] M. D. B. Charlton, S. W. Roberts, and G. J. Parker, Mater. Sci. Eng., B **49**, 155 (1997).
[4] A. Y. Vlasov, X. Bo, and C. J. Sturm, Nature (London) **6861**, 289 (2001).
[5] E. Özbay, E. Michel, and G. Tuttle, Appl. Phys. Lett. **64**, 2059 (1994).
[6] M. Campbell, N. D. Sharp, and T. M. Harrison, Nature (London) **6773**, 53 (2000).
[7] V. Y. Miklyaev, C. D. Meisel, and A. Blanco, Appl. Phys. Lett. **82**, 1284 (2003).
[8] D. N. Sharp, M. Campbell, and R. E. Dedman, Opt. Quantum Electron. **34**, 3 (2002).
[9] L. Z. Cai, X. L. Yang, and Y. R. Wang, J. Opt. Soc. Am. A **19**, 2238 (2002).
[10] I. Divliansky, T. S. Mayer, K. S. Holliday, and V. H. Crespi, Appl. Phys. Lett. **82**, 1667 (2003).
[11] G. Alagappan, X. W. Sun, P. Shum, and M. B. Yu, Opt. Lett. **31**, 1109 (2006).
[12] R. L. Sutherland, L. V. Natarajan, V. P. Tondiglia, and T. J. Bunning, Chem. Mater. **5**, 1533 (1993).
[13] K. Tanaka, K. Kato, M. Date, and S. Sakai, SID Int. Symp. Digest Tech. Papers **26**, 267 (1995).
[14] G. P. Crawford, T. G. Fiske, and L. D. Silverstein, SID Int. Symp. Digest Tech. Papers **27**, 99 (1996).
[15] T. J. Bunning, L. V. Natarajan, R. L. Sutherland, and V. P. Tondiglia, SID Int. Symp. Digest Tech. Papers **31**, 121 (2000).
[16] L. H. Domash, Y. M. Chen, B. Gomatam, C. Gozewski, R. L. Sutherland, L. V. Natarajan, V. P. Tondiglia, T. J. Bunning, and W. W. Adams, Proc. SPIE **2689**, 188 (1996).
[17] L. H. Domash, Y.-M. Chen, C. Gozewski, P. Haugsjaa, and M. Oren, Proc. SPIE **3010**, 214 (1997).
[18] Y. J. Liu, X. W. Sun, J. H. Liu, H. T. Dai, and K. S. Xu, Appl. Phys. Lett. **86**, 041115 (2005).
[19] D. E. Lucchetta, L. Criante, O. Francescangeli, and F. Simoni, Appl. Phys. Lett. **84**, 837 (2000).
[20] R. Jakubiak, V. P. Tondiglia, L. V. Natarajan, R. L. Sutherland, P. Lloyd, T. J. Bunning, and R. A. Vaia, Adv. Mater. (Weinheim, Ger.) **17**, 2807 (2005).
[21] Y. J. Liu, X. W. Sun, P. Shum, H. P. Li, J. Mi, W. Ji, and X. H. Zhang, Appl. Phys. Lett. **88**, 061107 (2006).
[22] M. J. Escuti, J. Qi, and G. P. Crawford, Appl. Phys. Lett. **83**, 1331 (2003).
[23] R. L. Sutherland, V. P. Tondiglia, L. V. Natarajan, and S. Chandra, Opt. Express **10**, 1074 (2002).
[24] V. P. Tondiglia, L. V. Natarajan, R. L. Sutherland, D. Tomlin, and T. J. Bunning, Adv. Mater. (Weinheim, Ger.) **14**, 187 (2002).
[25] M. J. Escuti and G. P. Crawford, Mol. Cryst. Liq. Cryst. **421**, 23 (2004).
[26] V. Berger, O. Gauthier-Lafaye, and E. Costard, Electron. Lett. **33**, 425 (1997).
[27] A three-index system of $(ab\bar{c})$ was used to represent the 2D hexagonal lattice, where $c=-(a+b)$.
[28] S. P. Gorkhali, J. Qi, and G. P. Crawford, J. Opt. Soc. Am. B **23**, 149 (2006).